Extracellular Matrix Remodeling by Dynamic Strain in a Three-Dimensional Tissue-Engineered Human Airway Wall Model

Melanie M. Choe, Peter H. S. Sporn, and Melody A. Swartz

Department of Biomedical Engineering, Northwestern University, Evanston; Division of Pulmonary and Critical Care Medicine, Feinberg School of Medicine, Northwestern University, Chicago, Illinois; and Institute of Bioengineering, École Polytechnique Fédérale de Lausanne (EPFL), Lausanne, Switzerland

Airway wall remodeling is a hallmark of asthma, characterized by subepithelial thickening and extracellular matrix (ECM) remodeling. Mechanical stress due to hyperresponsive smooth muscle cells may contribute to this remodeling, but its relevance in a three-dimensional environment (where the ECM plays an important role in modulating stresses felt by cells) is unclear. To characterize the effects of dynamic compression in ECM remodeling in a physiologically relevant three-dimensional environment, a tissue-engineered human airway wall model with differentiated bronchial epithelial cells atop a collagen gel containing lung fibroblasts was used. Lateral compressive strain of 10 or 30% at 1 or 60 cycles per hour was applied using a novel straining device. ECM remodeling was assessed by immunohistochemistry and zymography. Dynamic strain, particularly at the lower magnitude, induced airway wall remodeling, as indicated by increased deposition of types III and IV collagen and increased secretion of matrix metalloproteinase-2 and -9. These changes paralleled increased myofibroblast differentiation and were fibroblast-dependent. Furthermore, the spatial pattern of type III collagen deposition correlated with that of myofibroblasts; both were concentrated near the epithelium and decreased diffusely away from the surface, indicating some epithelial control of the remodeling response. Thus, in a physiologically relevant three-dimensional model of the bronchial wall, dynamic compressive strain induced tissue remodeling that mimics many features of remodeling seen in asthma, in the absence of inflammation and dependent on epithelial–fibroblast signaling.

Keywords: asthma; collagen; fibrosis; *in vitro*; myofibroblast

Remodeling of the airway wall in asthma is characterized by thickening of the subepithelial lamina reticularis, increase in smooth muscle mass, fibroblast hyperplasia, mucus hypersecretion, edema, and angiogenesis (1–6). The subepithelial fibrosis that is often part of this remodeling is further characterized by the differentiation of fibroblasts to myofibroblasts, which are more contractile than fibroblasts and are likely to contribute to the alignment and stiffening of the airway matrix by secretion of types I, III, and V collagen (7–14). In addition, matrix metalloproteinases (MMPs) and their inhibitors (tissue inhibitors of metalloproteinases [TIMPs]), particularly MMP-2 and -9 and TIMP-1, are also increased in the airways in asthma, as they are key players in extracellular matrix (ECM) remodeling (15, 16). Evidence from clinical studies supports the concept that airway remodeling contributes to irreversible airflow obstruction and loss of pulmonary function over time in patients with chronic asthma (17, 18).

The complex interplay of factors contributing to airway wall remodeling, which includes inflammatory and mechanical factors, is not well understood. Immune cells recruited to the inflamed airways release cytokines such as RANTES (CCL5), IL-13, TGF-β_1, and cysteinyl leukotrienes C4, D4, and E4 (19–21) that can stimulate epithelial cells, fibroblasts, and smooth muscle cells (SMCs). In asthma, the increase in SMC mass and hyperresponsiveness can result in amplified bronchoconstriction (22–25), which is associated with compressive stresses on the epithelial cells and fibroblasts (26, 27). These mechanical forces may then further contribute to airway remodeling (28, 29); for example, static compressive stress on epithelial cells can alter the expression of TGF-β_1, endothelin-1 (ET-1), early growth response-1 (Egr-1), epidermal growth factor receptor (EGFR) ligands, and fibronectin (30–33) (likely via an autocrine ligand signaling mechanism (34)), which may, in turn, activate fibroblasts to secrete matrix remodeling proteins (32). However, it is difficult to interpret the relevance of such stresses on matrix remodeling in the absence of a truly three-dimensional environment, where the ECM can (*1*) regulate cell–cell signaling by binding cytokines like RANTES (35) and growth factors like TGF-β_1 (36); (*2*) buffer mechanical stress via local heterogeneity in matrix properties (37); and (*3*) itself signal cells with soluble ECM fragments liberated during matrix remodeling. Indeed, such environmental factors may act to either augment or decrease the remodeling response by coordinating the various cell responses to stress (32). In addition, two-way cell–cell communication is critical for mediating overall remodeling responses, since fibroblasts and epithelial cells may each sense stress differently and play different roles in matrix remodeling. Clearly, the three-dimensional ECM is critical to modulating a stress environment to its resident cells, and thus the role of mechanical stress in airway wall remodeling cannot be definitively determined without a three-dimensional tissue environment.

In this study, we evaluate the effects of dynamic strain on matrix remodeling in a physiologically relevant three-dimensional tissue engineered human airway wall model. Several research groups, including our own, have recently demonstrated the advantages of three-dimensional airway co-culture models that provide an ECM and organization of a cellular community over traditional (two-dimensional, single-cell) culture models for recapitulating physiologic and pathophysiologic behavior (38–41). Our model here additionally mimics the mechanical function of the smooth muscle cells by incorporating lateral and dynamic compression to the three-dimensional culture system over a long-term period. We examine the effects of this mechanical strain on the airway wall with a focus on cell–cell and cell–matrix interactions. The results show that strain magnitudes of 10% and 30%, at frequencies of 1 and 60 cph, elicit selective responses in matrix

(*Received in original form December 3, 2005 and in final form March 31, 2006*)

This work was supported by the National Science Foundation (BES-0134551) and the National Institutes of Health (HL072891).

Correspondence and requests for reprints should be addressed to Melody A. Swartz, Ph.D., Integrative Biosciences Institute, SV - LMBM, Station 15, Ecole Polytechnique Fédérale de Lausanne (EPFL), 1015 Lausanne, Switzerland. E-mail: melody.swartz@epfl.ch

Am J Respir Cell Mol Biol Vol 35. pp 306–313, 2006
Originally Published in Press as DOI: 10.1165/rcmb.2005-0443OC on April 6, 2006
Internet address: www.atsjournals.org

remodeling that can be partly understood by the spatial deposition of ECM proteins with respect to cellular locations. In summary, we demonstrate that dynamic compression in our tissue engineered airway wall model can contribute to tissue remodeling similar to that seen in diseases such as asthma.

MATERIALS AND METHODS

Cell Culture

IMR-90 human fetal lung fibroblasts (HLF; ATCC, Manassas, VA) were used at passage 14–16 and cultured in α-MEM supplemented with 10% fetal bovine serum (Gibco BRL, Grand Island, NY) and 1% penicillin/streptomycin (Sigma, St. Louis, MO). Normal human bronchial epithelial cells (HBEC; Clonetics, Walkersville, MD) were expanded in bronchial epithelial growth medium (BEGM; Clonetics) supplemented with 50 nM retinoic acid (Sigma) and used at passage 3.

Detailed methods of culturing HLFs and HBECs and their characterization in three-dimensional collagen gels have been previously discussed (39). After cell expansion, each strain device (*see below*) was filled with a mixture of 5×10^5 cells/ml HLFs suspended in 2.5 mg/ml type I collagen isolated from rat tail tendon. The surface was then coated with an additional thin layer of acellular 2.5 mg/ml collagen before culture in media consisting of BEGM:DMEM (Gibco BRL) in a ratio of 1:1. After 2–4 h, HBECs were seeded on the surface at 2.5×10^5 cells/cm^2 (although some models were cultured without HBECs for fibroblast-only controls). The system was cultured in submersion for 7 d to allow HBECs to reach confluence, and in air–liquid interface (ALI) for another 7 d to allow differentiation of HBECs.

Strain Model and Characterization

We designed a dynamic strain culturing device (Figure 1) in which cells could be cultured to their differentiated state and then exposed to various amplitudes and frequencies of lateral dynamic strain to mimic the mechanical environment in constricting airway walls. The design included a strain applicator made of a Teflon frame, porous polyethylene (PE) ends to anchor the gel (both from Small Parts Inc., Miami Lakes, FL), and polyether sponge side linings threaded with 1-mm-diameter elastic bands for elastic recoil, with inner well dimensions of $40 \times 10 \times 5$ mm (Figure 1A). To support the tissue culture in ALI, a porous polycarbonate filter with 8-μm pores (Osmonics, Kent, WA) was attached to the bottom of the well with silicone glue. Static controls were cultured in devices that were identical, except that they had half the inner dimensions (to conserve cells).

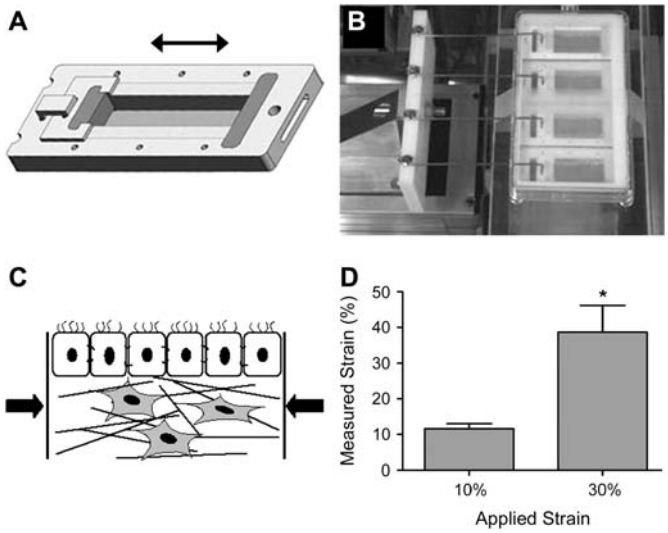

Figure 1. Dynamic strain model. (*A*) Individual wells with movable inner walls were designed to introduce lateral compressive strain to our three-dimensional human airway wall tissue models. (*B*) A computer-controlled motor-driven arm was coupled to the wells to impose the strain. (*C*) Lateral compression was introduced to the airway wall models. (*D*) The resulting strain, as measured by microbead displacement, was uniform throughout the length of the device, where applied strain of 10% and 30% at 60 cph translated to significantly different averages of 12% and 39% in gel, respectively (*$P = 0.001$); each was not significantly different from its applied strain of 10% and 30%.

To assemble the straining device, the sponge sides were fully extended to the length of the frame and clamped in place. Then collagen and cells were introduced to the model. After culture for 7 days submerged followed by 7 days in ALI in this expanded state, 10% or 30% compressive strain was imposed in the lateral direction at frequencies of 1 or 60 cph for a period of 48 h. This was achieved by releasing the clamp and applying strain (where compression was achieved by recoil of the elastic bands) via a computer-controlled, motor-driven mechanical arm (Figures 1B and 1C). The strain was applied in step fashion; that is, 1 cph consisted of ~ 30 min of compressive strain followed by 30 min without strain, and 60 cph consisted of 26 s of 10% compressive strain or 19 s of 30% strain followed by the same respective time without strain. In all cases, a ramping velocity of 1 mm/s (2.5% of original length per second) was used. Equivalent static controls were cultured in parallel with each experimental run. These magnitudes of strain were chosen according to published reports of ASM shortening in normal and asthmatic airways (24), and the frequencies were chosen as possible low and high bounds for frequency of ASM hyperactive episodes over a 48-h period.

The local distribution of strain within the three-dimensional matrix was determined in separate experiments using 10-μm-diameter fluorescent polystyrene microbeads (Molecular Probes, Eugene, OR), suspended at 250,000 beads/ml in the fibroblast-embedded collagen, at well-distributed points along the length of the gel before epithelial cell seeding. After the culturing protocol outlined in the previous section, strain was applied for a period of 24 h and three-dimensional images were obtained using confocal microscopy. Strain was estimated for discrete bead clusters in the direction of strain application by taking the change in distance in any two of these clusters (i.e., pre-strain distance minus strained distance) and dividing by their pre-strained distance. A total of three to six measurements were made throughout each gel ($n \geq 7$ for each strain level). In addition, the relative distribution of strain at different depths within the gel was determined by measuring the microbead density in four contiguous regions beneath the epithelium, each 88 μm in height ($n = 3$–6); this was assessed both before and after 24 h strain application of 10% or 30% strain at 1 cph for direct comparison between pre-strained and post-strained conditions.

Immunofluorescence

Ten-micrometer sections from paraffin-embedded samples, taken along the direction of applied strain, were stained with antibodies against human type III collagen (Oncogene, Boston, MA), type IV collagen (MP Biomedicals, Aurora, OH), fibronectin (Transduction Laboratories, Lexington, KY), and α-smooth muscle actin (α-SMA) (clone 1A4; Sigma). Standard immunostaining protocols were used, with 10% host serum (Dako, Glostrup, Denmark) of the secondary antibody used as a pre-staining block, biotinylated secondaries (Dako), and avidin-conjugated fluorescein for detection with DAPI-containing mounting medium (both from Vector Laboratories, Burlingame, CA). The relative amounts and spatial distributions of matrix proteins were analyzed using Metamorph software (Molecular Devices Corp., Downington, PA), and α-SMA expression was quantified by determining the percentage of nuclei with corresponding cytoplasmic staining for α-SMA.

Protease Analysis

Along with matrix deposition, increases in matrix metalloproteinases (MMPs) were examined after 48 h of strain application. For spatial distribution of MMP activity, *in situ* zymography was performed on cryosections (42). Briefly, unfixed thin cryosections were incubated in fluorescein-conjugated DQ-collagen type I (Molecular Probes) overnight in a dark humidified chamber at room temperature. Upon digestion or cleavage of the DQ-collagen substrate, the resulting fluorophore was excited at 495 nm and captured using an epifluorescence microscope. Additionally, MMP-2 and -9 released into the media were detected with gel zymography. Media collected at the end of experiments

were run on gelatin-containing zymogram gels (BioRad, Hercules, CA), a substrate for many MMPs, including MMP-2 and -9, in a standard vertical mini-electrophoresis cell. The gels were then renatured for 30 min at room temperature, developed overnight at 37°C, counterstained in 0.5 wt% Coomassie blue, and destained (all solutions from BioRad). Pictures were captured using Kodak DC290 (Kodak, New Haven, CT), and band intensities analyzed with ImageJ (NIH, Bethesda, MD).

Statistical Analysis

Results are expressed as mean and standard error of at least eight samples per condition. Mean (± SEM) values were compared using one-way ANOVA with Tukey *post hoc* analysis, and considered significant for P values < 0.05.

RESULTS

Model Characterization

With an applied lateral strain of 10% and 30%, the local strain within the collagen gel, as measured by microbead displacements, translated to 11.6 ± 1.4% and 38.7 ± 7.6%, respectively (Figure 1D). They were significantly different from each other (using a *t* test) but there was no significant difference between measured and applied strains. No relationship between bead position and measured strain could be detected, implying uniform strain throughout the gel.

Epithelial differentiation and cellular organization in the airway wall model were consistent with our previous findings in a similar unstrained model, which we adapted for the current study (39). We observed tightly packed and ciliated epithelial cells after 10 d of ALI (Figures 2A–2B) that were active in synthesizing mucins (Figure 2C). The cells were well organized, with a pseudostratified layer of epithelial cells on the apical surface, and individual fibroblasts spread sparsely throughout the matrix below (Figure 2D). These features replicate the anatomic relationships of HBECs and HLFs in the airway *in vivo*, and therefore establish the physiologic relevance of our tissue-engineered airway wall model.

ECM Protein Deposition

ECM proteins that are typically seen in remodeled airways include types III and IV collagen and fibronectin (Figure 3). We found that in our tissue engineered airway wall model, deposition of type III collagen increased with all levels of dynamic strain, except 30% strain at 60 cph, which, interestingly, was the highest strain and frequency applied. For type IV collagen, we saw similar trends in that the lower magnitude (10%) was more effective at increasing ECM deposition than the higher magnitude of strain. In contrast, fibronectin deposition was decreased with all levels of strain compared with static controls. None of these ECM proteins were detected in acellular samples (data not shown), indicating that they were all cell-derived.

We also saw qualitative differences in the deposition patterns of these proteins between strained and static samples (Figure 3). While type III collagen in the static control was expressed uniformly throughout the matrix and in layers aligned parallel to the surface (Figure 3A), strained samples showed higher levels just beneath the epithelium with a decreasing gradient away from the surface (Figure 3B). In contrast, type IV collagen appeared as punctate strands extended in the horizontal direction and localized around the fibroblasts (Figures 3D and 3E). Furthermore, an increased amount of type IV collagen was deposited just beneath the epithelium in strained samples (Figure 3E), although the spatial gradient in expression was not as pronounced as that seen for type III collagen (Figure 3E). Finally, fibronectin distribution was similar to that of type IV collagen, with obvious staining of the basement membrane (Figures 3G and 3H), but no differences were detected in the spatial distribution of fibronectin in any of the conditions.

Quantitative analyses of ECM immunofluorescent stainings confirmed that types III and IV collagen (Figures 3C and 3F) were significantly increased with strain at all levels except the highest strain conditions (30% at 60 cph for type III collagen and 30% at both frequencies for type IV collagen). In addition, fibronectin was decreased by dynamic strain at all levels (Figure 3I). To assess the relevance of epithelial signaling in fibroblast remodeling of these proteins, fibroblast-only experiments were performed at the 10%, 1 cph condition. We found that strain did significantly upregulate type III collagen in fibroblast-only cultures (Figure 3C), although the levels of total protein were much lower at both unstrained and strained conditions than in all co-culture conditions. In contrast, type IV collagen was not significantly affected by strain in fibroblast-only cultures (Figure 3F). Finally, fibronectin remodeling was similar in fibroblast-only compared with co-culture conditions (Figure 3I). Thus, these data indicate that epithelial signaling (*1*) dominates the strain-induced remodeling response of type IV collagen, (*2*) strongly affects the strain-induced increase of type III collagen, and (*3*) does not affect strain-induced remodeling of fibronectin, which appears to be solely controlled by fibroblasts alone.

Protease Secretion

ECM degradation by metalloproteinases is an important component of tissue remodeling. We therefore examined the spatial distribution of collagenolytic activity in cryosections of the airway wall model by *in situ* zymography and specifically assessed the activity of MMP-2 and -9 secreted into culture medium by electrophoresis and gelatin zymography (Figure 4). Representative *in situ* zymograms, comparing static versus strained (10% at 60 cph) samples, are shown in Figure 4A. Collagenolytic activity in the epithelium and around fibroblasts was increased by mechanical strain. Interestingly, collagenolytic activity beneath the epithelium was distributed in a horizontal orientation, similar to that of the fibroblasts themselves.

Gelatin zymography was performed on conditioned medium after each experiment (Figure 4B), and bands were detected at 62, 72, and 92 kD, corresponding to the active form of MMP-2 and latent forms of MMP-2 and -9, respectively. In fibroblast-only cultures, only active and latent forms of MMP-2 were present. Quantification of the band intensities verified that these MMP levels were increased with all levels of strain, with MMP-9 being the most strain-sensitive (Figure 4C). We also verified that the increased levels of MMPs were not simply due to their release from the interstitial space under a one time compression of 50%, which gave similar results as unstrained samples (data not shown).

Myofibroblast Differentiation

Fibroblast-to-myofibroblast differentiation is an important contributor to airway wall remodeling (43). Myofibroblasts are characterized by expression of α-SMA, which is associated with the contractile phenotype of these cells and may contribute to airway narrowing by an increased capacity for ECM protein synthesis (12). We found that 10% strain increased myofibroblast differentiation (quantified by number of α-SMA–positive cells) compared with static controls (Figure 5). Interestingly, this effect was not seen with 30% strain. Thus, like type IV collagen deposition, increased myofibroblast differentiation was only seen in low-strain samples.

Spatial Distribution of Remodeling

As noted in Figures 3 and 5, the deposition of types III and IV collagen and myofibroblast differentiation were concentrated

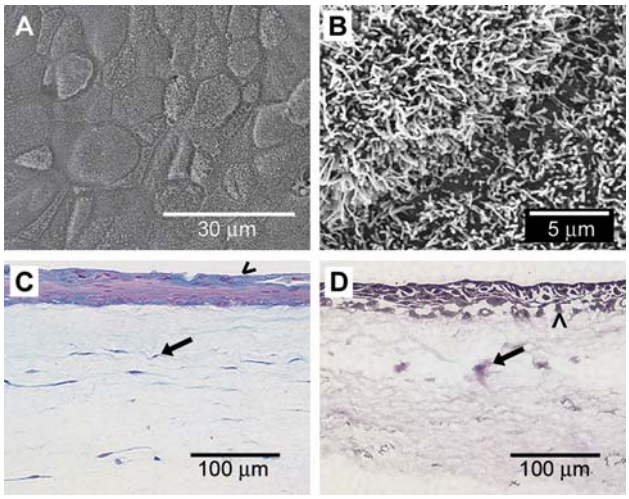

Figure 2. Morphologic features of the three-dimensional human airway wall model. (*A*) SEM of the apical surface reveals a tightly packed epithelium. (*B*) Under higher magnification in SEM, a dense carpet of cilia is observed. (*C*) Alcian blue staining shows mucin production (*blue*) by epithelial cells (*arrowhead*); fibroblasts are uniformly distributed within the subepithelial tissue (*arrow*) with all nuclei in red. (*D*) Van Gieson and hematoxylin stains show fibroblasts (*arrow*) distributed throughout the collagen matrix beneath the epithelial layer (*arrowhead*).

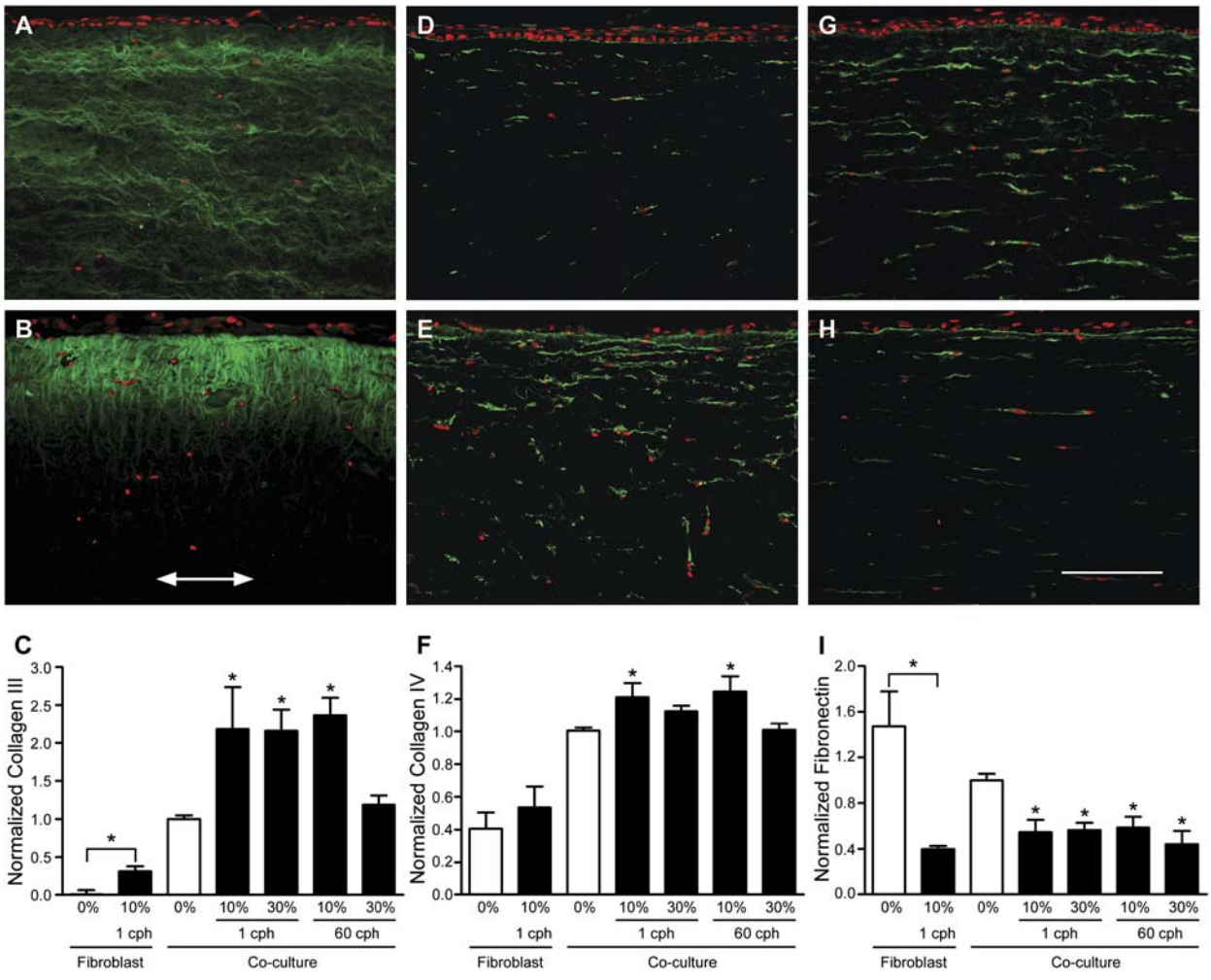

Figure 3. Extracellular matrix protein deposition was altered by dynamic mechanical strain. All images show 10-μm paraffin-embedded sections, immunostained for types III collagen, IV collagen, and fibronectin (all in *green*), with a *red* nuclear counterstain; *arrow* indicates direction of strain and *bar* = 150 μm. *Top row* shows representative co-culture images from unstrained controls, while the *middle row* shows representative co-culture images from 10% strain, 1 cph. The *bottom row* shows the image intensity analysis averaged for all fibroblast-only and co-culture samples. (*A*) Type III collagen in unstrained versus (*B*) strained samples, where deposition was highest just beneath the epithelium and decreased with depth into the tissue (*arrow* indicates strain direction). (*C*) Type III collagen upregulation was greater for all strain levels except the highest strain rate applied (30% at 60 cph) in both fibroblast only and co-culture systems when compared with their respective static controls. (*D*) Type IV collagen expression in unstrained versus (*E*) strained samples, where deposition was also highest near the epithelium and decreased with depth. (*F*) Significant increase in type IV collagen was seen only with 10% strain in co-cultures. (*G*) Fibronectin production in unstrained versus (*H*) strained samples, where production was noticeably decreased. (*I*) Fibronectin quantification showed a significant decrease with all levels of strain and in the presence of the epithelium. *$P < 0.05$ compared with respective static controls.

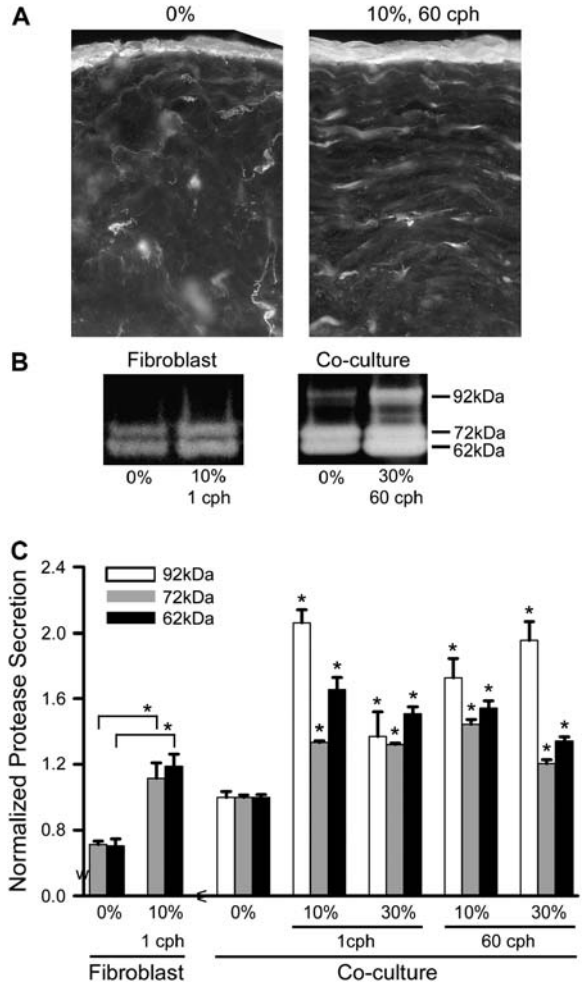

Figure 4. Overall protease activity increased with all levels of strain. (*A*) *In situ* zymography on 25-μm cryosections show protease activity concentrated in the epithelium and around fibroblasts. (*B*) Representative gel zymograms from strained (10%, 1 cph) fibroblast-only versus co-culture models show bands at 62, 72, and 92 kD, corresponding to active MMP-2, pro–MMP-2, and pro–MMP-9, respectively. All were visibly increased with strain; in models with only fibroblasts, the 92-kD band was missing, indicating that the epithelial cells were critical in the release of pro–MMP-9. (*C*) Zymogram quantification demonstrates significant increases in proteolysis in all levels of strain normalized to their respective static controls. Static fibroblast-only samples showed no detectable MMP-9 and released ~ 25% less MMP-2 than static co-cultures. *$P < 0.05$ compared with respective static controls.

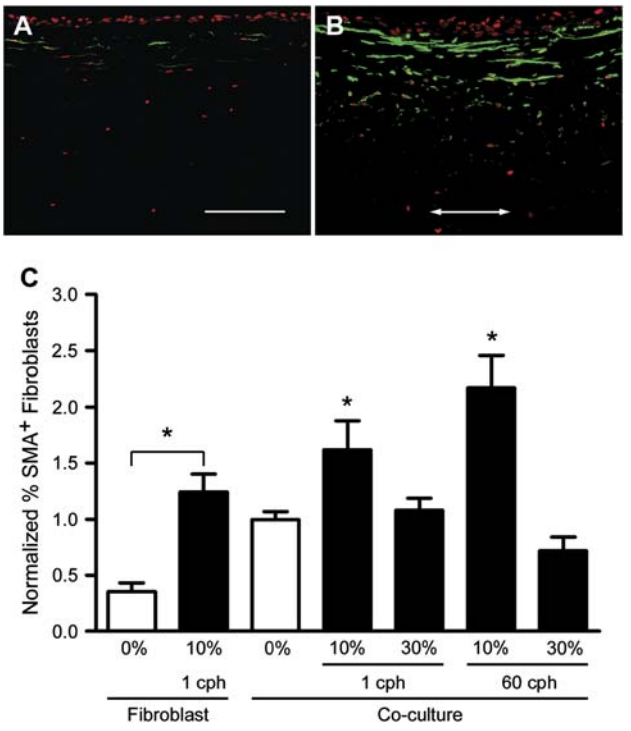

Figure 5. Myofibroblast differentiation increased with 10% strain. Representative (*A*) static and (*B*) strained (10%, 1 cph) sections from co-cultures show the upregulation of α-SMA+ cells (*green* with *red* nuclear counterstain), particularly close to the epithelium, by dynamic strain. *Arrow* indicates direction of strain (*bar* = 150 μm). (*C*) Quantification of α-SMA+ cells demonstrates that 10% strain caused significant increases in α-SMA expression compared with respective static controls; cell differentiation was increased by 62% at 1 cph and by 117% at the higher frequency of 60 cph. *$P < 0.05$ compared with respective static controls.

just beneath the epithelium and decreased with increasing distance from the epithelium. To quantify this spatial distribution, the sections were divided into four contiguous regions, each of 88 μm in depth, beneath the epithelium (Figures 6A and 6C). This revealed that the density in the number of myofibroblasts (Figure 6B), as well as the intensity of type III collagen staining (Figure 6D), was significantly greater just beneath the epithelium than in any other region of the tissue. Furthermore, although this increase near the epithelium was seen in both static and strained co-culture samples, the gradient was amplified by strain: over 50% more expression of myofibroblasts and type III collagen was found in region I than the other regions for 10% strain (in the case of myofibroblasts) and all levels of strain except the highest strain rate (in the case of type III collagen) in co-cultures. This highlights the importance of epithelial–fibroblast communication in remodeling.

We note that these spatial gradients were not due to nonuniform strain distribution at different depths within the gel. The *inset graph* in Figure 6D shows the difference in microbead density before and after strain, normalized to respective region I for direct comparison, which shows no significant differences among the four regions, implying a uniform distribution of strain. In fibroblast-alone systems, while 10% strain at 1 cph resulted in an overall increase of myofibroblast expression in all regions, no gradient in expression was observed for both myofibroblast and type III collagen, indicating a role for epithelial–fibroblast signaling in strain-induced remodeling in the co-culture system. Similar results were found by analyzing regional intensities for type IV collagen expression (data not shown). Thus, strain-induced matrix production was largely controlled by signals from the epithelium as evidenced by increased remodeling near (and below) the epithelium, where myofibroblasts were found in abundance.

DISCUSSION

As the importance of the microenvironment in governing cell responses has been demonstrated in numerous examples, three-dimensional tissue models are proving to be invaluable to studying cell and tissue physiology and pathophysiology (44, 45). As such, there is a growing appreciation for the importance of

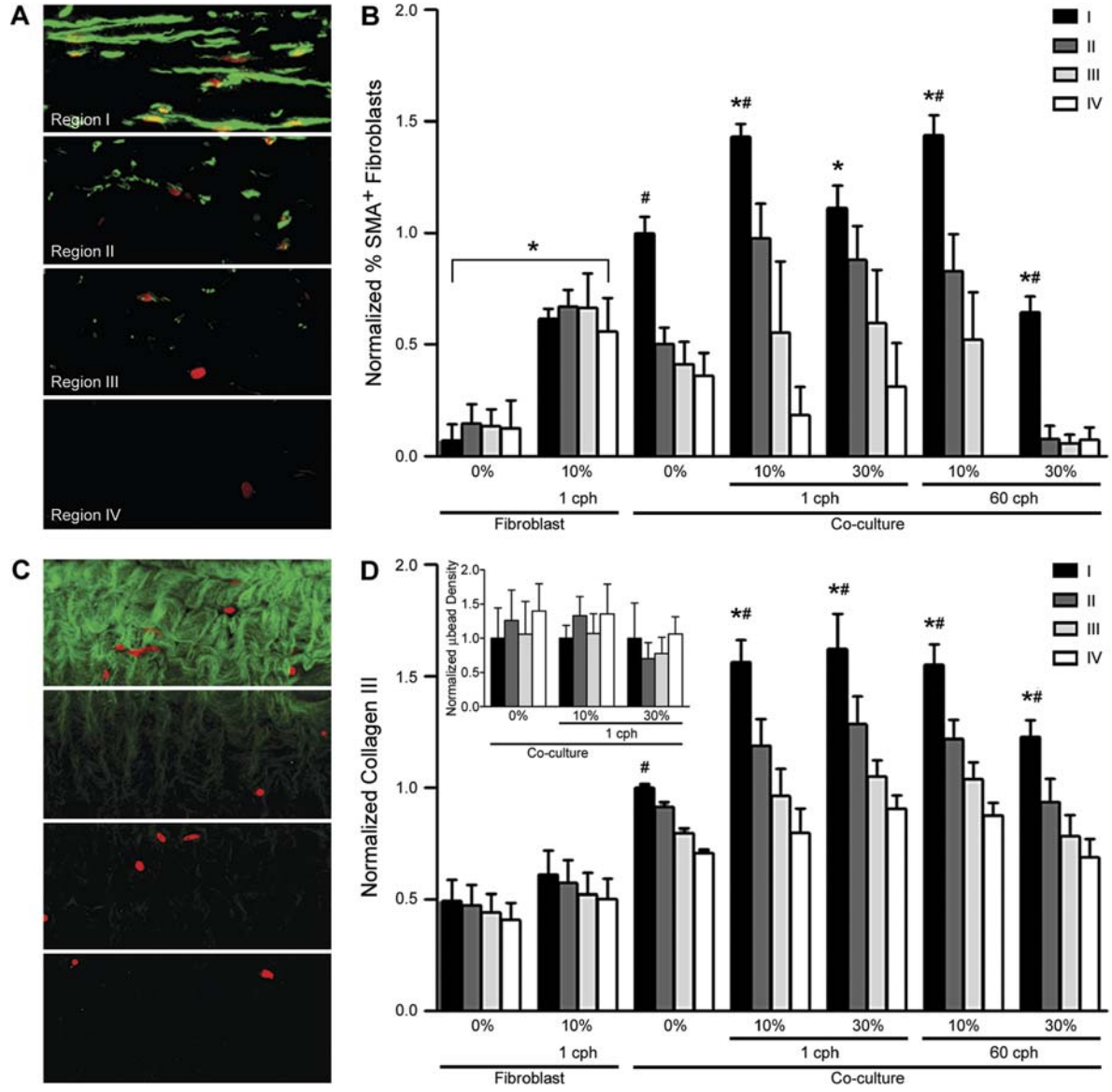

Figure 6. The spatial distribution of myofibroblasts generally correlated with the spatial distribution of type III collagen deposition and was concentrated close to the basal side of the epithelium. (*A*) Immunostained thin sections were divided into four equal regions for intensity analysis as shown for α-SMA; each region had a depth of 88 μm. (*B*) Myofibroblasts, as detected by α-SMA expression, were found in greater numbers in region I, and diminished in regions farther away from the epithelium. Furthermore, only 10% strain resulted in significantly greater myofibroblast expression compared with region I in static control co-cultures. In fibroblast-only cultures, 10% strain resulted in a uniform increase of α-SMA expression. (*C*) Likewise, thin sections were immunostained for type III collagen and divided into equal regions. (*D*) Type III collagen production was also significantly increased in region I near the epithelium under all conditions, and all strain conditions resulted in significantly greater production in region I as compared with static controls for co-cultures. Regional difference in type III collagen production was not observed in fibroblast-only cultures. The *inset bar graph* shows uniform distribution of microbeads throughout various depths in co-cultures in the presence and absence of strain. $^{*}P < 0.01$ compared with respective static controls and $^{\#}P < 0.05$ compared with respective regions II–IV.

the biophysical environment, with appropriate mechanical cues, in both making the three-dimensional models more physiologic and also in studying the roles of such cues in pathophysiology (37). Our results, using a physiologically relevant three-dimensional tissue model of the human airway wall, demonstrate the importance of mechanical stress in airway wall remodeling and the importance of epithelial–fibroblast crosstalk in such remodeling.

Our *in vitro* tissue model showed physiologically relevant cell organization and function: it has a pseudostratified epithelium with both ciliated and mucus-producing cells, and under baseline culturing conditions secreted basement membrane beneath the epithelium and type III collagen and fibronectin, among other matrix proteins, within the tissue.

SMCs were absent in our model, which is important to consider in interpreting overall remodeling response, since they can also secrete molecular regulators of airway wall remodeling and fibroblast differentiation (23, 25). However, their mechanical function was simulated by inducing lateral dynamic strain with a custom-made strain device. It has been reported in computational models of airway mechanics in asthma that 40% shortening of the airway smooth muscle (ASM) can result in almost total occlusion of the airway (26), while in others, 30% shortening

may translate to a > 15-fold increase in pulmonary resistance in asthmatic versus normal airways (46, 47). In additionally, isolated human bronchial smooth muscle cells from individuals with asthma were found to contract to a greater extent—more than 10% in length—compared with cells from normal subjects (24). In light of these results, we chose 10% and 30% as representative strain magnitudes of ASM shortening.

In addition to strain magnitude, the duration and frequency of ASM contraction were important parameters to consider. While it is difficult to generalize the transient behavior of smooth muscle contraction, several studies have shown with isolated human bronchial ASM cells (24) and canine muscle strips (48) that 75% of their contractions are completed within 1.5–4 s. The time we imposed for contraction was $\sim$ 4 s for 10% strain and $\sim$ 12 s for 30% strain. In addition, frequency may also be an important factor in remodeling, but the duration of ASM hyperactivity can vary dramatically for individuals with asthma with variation in severity; thus it is difficult again to generalize the relevant frequencies to use for *in vitro* simulations. We chose 1 and 60 cph as possible low and high frequencies of ASM contraction over a 48-h period. Therefore, with these parameters, we attempted to represent reasonably relevant values of strain that may contribute to ECM remodeling.

In our three-dimensional model, strain influenced cell–matrix and cell–cell interactions to change the architecture and organization of the ECM in the absence of inflammation. The deposition of types III and IV collagen was concentrated near the epithelium and decreased away from the epithelium, which was not observed in fibroblast-only conditions. The epithelium may play an important role as a source of profibrotic mediators such as TGF-β_1 leading to matrix remodeling (8, 10). Furthermore, the spatial gradient in ECM protein deposition was amplified under all strain conditions compared with static controls (Figure 6D, data not shown for type IV collagen), suggesting that epithelial–fibroblast communication, possibly aided by convection of secreted mediators, may act to facilitate the spatial deposition of these ECM proteins.

While this study examined only a few ECM proteins, our results correlate with remodeling characteristics seen in the human airways. In individuals with asthma, the subepithelial layer of the airway wall is thickened and enriched with types III and IV collagen, as well as type V collagen, fibronectin, and tenascin (1, 49, 50). Consistent with such pathologic remodeling, we observed deposition of types III and IV collagen concentrated in the subepithelial region and amplified with dynamic strain in our model. Interestingly, we found that strain decreased fibronectin deposition, indicating differential regulation of various ECM proteins in response to mechanical strain.

In addition to HBECs and HLFs, myofibroblasts may have contributed to collagen production in our system. Myofibroblasts are commonly found in the thickened subepithelial collagen layer of the asthmatic airway wall (7, 14), and in the lungs of patients with pulmonary fibrosis (43). They play an important part in remodeling by matrix contraction (12, 51) and synthesis of types I and III collagen (52). In our system, myofibroblasts were found in increased numbers just beneath the epithelium, in the same spatial distribution as type III collagen under conditions of mechanical strain (Figure 6B and D). These results suggest that myofibroblasts were likely an important cellular source of collagen synthesis in response to mechanical strain.

In conclusion, we have shown that mechanical strain in a tissue engineered three-dimensional co-culture model of the airway wall can be an important determinant of ECM remodeling, as indicated by deposition/secretion of ECM proteins and MMPs, and by differentiation of myofibroblasts. In our three-dimensional airway wall model, we found lateral compressive strain on airway cells resulted in upregulation of types III and IV collagen and increased levels of secreted MMP-2 and -9, but downregulation of fibronectin. In addition, type III collagen was spatially correlated with myofibroblast differentiation. Thus, our dynamic human airway wall model demonstrates the importance of mechanical strain in airway wall remodeling in a relevant three-dimensional environment, independent of inflammatory cells and their mediators.

***Conflict of Interest Statement*:** None of the authors has a financial relationship with a commercial entity that has an interest in the subject of this manuscript.

***Acknowledgments*:** The authors thank Tom Keimig and Cara-Lynn Helm for their invaluable technical assistance.

References

1. James A. Airway remodeling in asthma. *Curr Opin Pulm Med* 2005;11: 1–6.
2. Homer RJ, Elias JA. Airway remodeling in asthma: therapeutic implications of mechanisms. *Physiology (Bethesda)* 2005;20:28–35.
3. Cohn L, Elias JA, Chupp GL. Asthma: mechanisms of disease persistence and progression. *Annu Rev Immunol* 2004;22:789–815.
4. McParland BE, Macklem PT, Pare PD. Airway wall remodeling: friend or foe? *J Appl Physiol* 2003;95:426–434.
5. Jeffery PK. Remodeling in asthma and chronic obstructive lung disease. *Am J Respir Crit Care Med* 2001;164:S28–S38.
6. Kumar RK. Understanding airway wall remodeling in asthma: a basis for improvements in therapy? *Pharmacol Ther* 2001;91:93–104.
7. Larsen K, Malmstrom J, Wildt M, Dahlqvist C, Hansson L, Marko-Varga G, Bjermer L, Scheja A, Westergren-Thorsson G. Functional and phenotypical comparison of myofibroblasts derived from biopsies and bronchoalveolar lavage in mild asthma and scleroderma. *Respir Res* 2006;7:11.
8. Boxall C, Holgate ST, Davies DE. The contribution of transforming growth factor-beta and epidermal growth factor signalling to airway remodelling in chronic asthma. *Eur Respir J* 2006;27:208–229.
9. Pepe C, Foley S, Shannon J, Lemiere C, Olivenstein R, Ernst P, Ludwig MS, Martin JG, Hamid Q. Differences in airway remodeling between subjects with severe and moderate asthma. *J Allergy Clin Immunol* 2005;116:544–549.
10. Kelly MM, Leigh R, Bonniaud P, Ellis R, Wattie J, Smith MJ, Martin G, Panju M, Inman MD, Gauldie J. Epithelial expression of profibrotic mediators in a model of allergen-induced airway remodeling. *Am J Respir Cell Mol Biol* 2005;32:99–107.
11. Johnson PRA, Burgess JK. Airway smooth muscle and fibroblasts in the pathogenesis of asthma. *Curr Allergy Asthma Rep* 2004;4:102–108.
12. Gabbiani G. The myofibroblast in wound healing and fibrocontractive diseases. *J Pathol* 2003;200:500–503.
13. Hashimoto S, Gon Y, Takeshita I, Matsumoto K, Maruoka S, Horie T. Transforming growth factor-β1 induces phenotypic modulation of human lung fibroblasts to myofibroblast through a c-jun-NH2-terminal kinase-dependent pathway. *Am J Respir Crit Care Med* 2001;163:152–157.
14. Brewster CE, Howarth PH, Djukanovic R, Wilson J, Holgate ST, Roche WR. Myofibroblasts and subepithelial fibrosis in bronchial asthma. *Am J Respir Cell Mol Biol* 1990;3:507–511.
15. Chakrabarti S, Patel KD. Matrix metalloproteinase-2 (MMP-2) and MMP-9 in pulmonary pathology. *Exp Lung Res* 2005;31:599–621.
16. Atkinson JJ, Senior RM. Matrix metalloproteinase-9 in lung remodeling. *Am J Respir Cell Mol Biol* 2003;28:12–24.
17. Ten Hacken NHT, Postma DS, Timens W. Airway remodeling and long-term decline in lung function in asthma. *Curr Opin Pulm Med* 2003;9: 9–14.
18. Rasmussen F, Taylor DR, Flannery EM, Cowan JO, Greene JM, Herbison GP, Sears MR. Risk factors for airway remodeling in asthma manifested by a low postbronchodilator FEV1/vital capacity ratio: a longitudinal population study from childhood to adulthood. *Am J Respir Crit Care Med* 2002;165:1480–1488.
19. Pease JE. Asthma, allergy and chemokines. *Curr Drug Targets* 2006;7: 3–12.
20. Perng DW, Wu YC, Chang KT, Wu MT, Chiou YC, Su KC, Perng RP, Lee YC. Leukotriene C-4 induces TGF-β1 production in airway epithelium via p38 kinase pathway. *Am J Respir Cell Mol Biol* 2006; 34:101–107.
21. Beller TC, Friend DS, Maekawa A, Lam BK, Austen KF, Kanaoka Y. Cysteinyl leukotriene 1 receptor controls the severity of chronic

pulmonary inflammation and fibrosis. *Proc Natl Acad Sci USA* 2004; 101:3047–3052.
22. Woodruff PG, Dolganov GM, Ferrando RE, Donnelly S, Hays SR, Solberg OD, Carter R, Wong HH, Cadbury PS, Fahy JV. Hyperplasia of smooth muscle in mild to moderate asthma without changes in cell size or gene expression. *Am J Respir Crit Care Med* 2004;169:1001–1006.
23. Fredberg JJ. Bronchospasm and its biophysical basis in airway smooth muscle. *Respir Res* 2004;5:2.
24. Ma X, Cheng Z, Kong H, Wang Y, Unruh H, Stephens NL, Laviolette M. Changes in biophysical and biochemical properties of single bronchial smooth muscle cells from asthmatic subjects. *Am J Physiol Lung Cell Mol Physiol* 2002;283:L1181–L1189. (comment).
25. Black JL, Roth M, Lee J, Carlin S, Johnson PRA. Mechanisms of airway remodeling - Airway smooth muscle. *Am J Respir Crit Care Med* 2001; 164:S63–S66.
26. Seow CY, Wang L, Pare PD. Airway narrowing and internal structural constraints. *J Appl Physiol* 2000;88:527–533.
27. Wiggs BR, Hrousis CA, Drazen JM, Kamm RD. On the mechanism of mucosal folding in normal and asthmatic airways. *J Appl Physiol* 1997;83:1814–1821.
28. Tschumperlin DJ, Drazen JM. Chronic effects of mechanical force on airways. *Annu Rev Physiol* 2006;68:563–583.
29. Tepper RS, Ramchandani R, Argay E, Zhang L, Xue Z, Liu Y, Gunst SJ. Chronic strain alters the passive and contractile properties of rabbit airways. *J Appl Physiol* 2005;98:1949–1954.
30. Chu EK, Foley JS, Cheng J, Patel AS, Drazen JM, Tschumperlin DJ. Bronchial epithelial compression regulates epidermal growth factor receptor family ligand expression in an autocrine manner. *Am J Respir Cell Mol Biol* 2005;32:373–380.
31. Tschumperlin DJ, Shively JD, Kikuchi T, Drazen JM. Mechanical stress triggers selective release of fibrotic mediators from bronchial epithelium. *Am J Respir Cell Mol Biol* 2003;28:142–149.
32. Swartz MA, Tschumperlin DJ, Kamm RD, Drazen JM. Mechanical stress is communicated between different cell types to elicit matrix remodeling. *Proc Natl Acad Sci USA* 2001;98:6180–6185.
33. Ressler B, Lee RT, Randell SH, Drazen JM, Kamm RD. Molecular responses of rat tracheal epithelial cells to transmembrane pressure. *Am J Physiol Lung Cell Mol Physiol* 2000;278:L1264–L1272.
34. Tschumperlin DJ, Dai GH, Maly IV, Kikuchi T, Laiho LH, McVittie AK, Haley KJ, Lilly CM, So PTC, Lauffenburger DA, *et al.* Mechanotransduction through growth-factor shedding into the extracellular space. *Nature* 2004;429:83–86.
35. Patel DD, Koopmann W, Imai T, Whichard LP, Yoshie O, Krangel MS. Chemokines have diverse abilities to form solid phase gradients. *Clin Immunol* 2001;99:43–52.
36. Unsold C, Hyytiainen M, Bruckner-Tuderman L, Keski-Oja J. Latent TGF-beta binding protein LTBP-1 contains three potential extracellular matrix interacting domains. *J Cell Sci* 2001;114:187–197.
37. Pedersen JA, Swartz MA. Mechanobiology in the third dimension. *Ann Biomed Eng* 2005;33:1–11.
38. Paquette JS, Moulin V, Tremblay P, Bernier V, Boutet M, Laviolette M, Auger FA, Boulet LP, Goulet F. Tissue-engineered human asthmatic bronchial equivalents. *Eur Cell Mater* 2004;7:1–11. (discussion 11–11).
39. Choe MM, Sporn PHS, Swartz MA. An in vitro airway wall model of remodeling. *Am J Physiol Lung Cell Mol Physiol* 2003;285:L427–L433.
40. Chakir J, Page N, Hamid Q, Laviolette M, Boulet LP, Rouabhia M. Bronchial mucosa produced by tissue engineering: a new tool to study cellular interactions in asthma. *J Allergy Clin Immunol* 2001;107:36–40.
41. Agarwal A, Coleno ML, Wallace VP, Wu WY, Sun CH, Tromberg BJ, George SC. Two-photon laser scanning microscopy of epithelial cell-modulated collagen density in engineered human lung tissue. *Tissue Eng* 2001;7:191–202.
42. Oh LYS, Larsen PH, Krekoski CA, Edwards DR, Donovan F, Werb Z, Yong VW. Matrix metalloproteinase-9/gelatinase B is required for process outgrowth by oligodendrocytes. *J Neurosci* 1999;19:8464–8475.
43. Phan SH. The myofibroblast in pulmonary fibrosis. *Chest* 2002;122:286s–289s.
44. Griffith LG, Swartz MA. Capturing complex 3D tissue physiology in vitro. *Nat Rev Mol Cell Biol* 2006;7:211–224.
45. Lysaght MJ, Hazlehurst AL. Tissue engineering: the end of the beginning. *Tissue Eng* 2004;10:309–320.
46. James AL, Pare PD, Hogg JC. The mechanics of airway narrowing in asthma. *Am Rev Respir Dis* 1989;139:242–246.
47. Pare PD, Wiggs BR, James A, Hogg JC, Bosken C. The comparative mechanics and morphology of airways in asthma and in chronic obstructive pulmonary disease. *Am Rev Respir Dis* 1991;143:1189–1193.
48. Stephens NL, Wang Y, Li W, Ma X. Airway hyperreactivity: direct smooth muscle approach. *Pulm Pharmacol Ther* 1999;12:97–101.
49. James AJ. Relationship between airway wall thickness and airway hyperresponsiveness. In: Stewart AG, editor. Airway wall remodeling in asthma. Boca Raton: CRC Press; 1997. pp. 1–27.
50. Roche WR, Beasley R, Williams JH, Holgate ST. Subepithelial fibrosis in the bronchi of asthmatics. *Lancet* 1989;1:520–524.
51. Tomasek JJ, Gabbiani G, Hinz B, Chaponnier C, Brown RA. Myofibroblasts and mechano-regulation of connective tissue remodelling. *Nat Rev Mol Cell Biol* 2002;3:349–363.
52. Hastie AT, Kraft WK, Nyce KB, Zangrilli JG, Musani AI, Fish JE, Peters SP. Asthmatic epithelial cell proliferation and stimulation of collagen production - Human asthmatic epithelial cells stimulate collagen type III production by human lung myofibroblasts after segmental allergen challenge. *Am J Respir Crit Care Med* 2002;165:266–272.